Building and Environment 72 (2014) 287–299

Contents lists available at ScienceDirect

Building and Environment

journal homepage: www.elsevier.com/locate/buildenv

Coupling a neural network temperature predictor and a fuzzy logic controller to perform thermal comfort regulation in an office building

Antonino Marvuglia [a], Antonio Messineo [b,*], Giuseppina Nicolosi [b]

[a] Public Research Centre Henri Tudor (CRPHT), Resource Centre for Environmental Technologies (CRTE), 6A, Avenue des Hauts-Fourneaux, L-4362 Esch-sur-Alzette, Luxembourg

[b] Faculty of Engineering and Architecture, University of Enna "Kore", Cittadella Universitaria, 94100 Enna, Italy

ARTICLE INFO

Article history:
Received 21 May 2013
Received in revised form
2 October 2013
Accepted 30 October 2013

Keywords:
Indoor thermal comfort
Artificial neural networks
NNARX
Fuzzy logic
Controller
Temperature forecast

ABSTRACT

The paper describes the application of a combined neuro-fuzzy model for indoor temperature dynamic and automatic regulation. The neural module of the model, an auto-regressive neural network with external inputs (NNARX), produces indoor temperature forecasts that are used to feed a fuzzy logic control unit that simulates switching the heating, ventilation and air conditioning (HVAC) system on and off and regulating the inlet air speed. To generate an indoor temperature forecast, the NNARX module uses weather parameters (e.g., outdoor temperature, air relative humidity and wind speed) and the indoor temperature recorded in previous time steps as regressors. In its current state, the fuzzy controller is only driven by the indoor temperature forecasted by the NNARX module; no variations in indoor heat gains or occupants' clothing and behavior were considered for driving the controller.

The main goal of this paper is to demonstrate the effectiveness of the hybrid neuro-fuzzy approach and the importance of efficiently designing the temperature forecast model, especially with respect to the selection of the *order* of the regressor for each of the external and internal parameters used. Therefore, a differential entropy-based method was applied in this study, which provided good forecasting performances for the NNARX model.

1. Introduction

Considering that we spend more of our time indoors as we become more affluent, over the last few decades, the problem of indoor air quality in non-industrial environments (particularly in dwellings and offices) has gained significant importance in relation to the effects on human health. In fact, it is estimated that during a normal weekday (excluding holidays), we now spend over 90% of our time indoors [1]. The air quality in working environments, dwellings and open space urban environments, is increasingly perceived by the public as one determinant of quality of life. Moreover, poor indoor comfort has direct effects on user productivity and indirect effects on building energy efficiency [2,3].

Temperature control represents one of the strategies to attain individual comfort in indoor environments, although temperature is only one of the factors affecting the thermal comfort level. ISO regulation 7730 defines thermal comfort as "the condition of mind that expresses satisfaction with the thermal environment and is assessed by subjective evaluation" [4]. Moreover, the ANSI/ASHRAE 55-2010 standards define the thermally acceptable environmental conditions for the occupants of indoor environments and suggest temperatures[1] and airflow rates in different types of buildings and different environmental circumstances [5].

The operative temperature intervals vary by indoor location type. ASHRAE suggests temperature ranges and airflow rates in different types of buildings and different environmental conditions. For example, for a single office in a building (with an occupancy ratio per square meter of 0.1) in the summer, the suggested temperature range is between 23.5 and 25.5 °C; the airflow velocity is recommended to be 0.18 m/s. In the winter, the recommended temperature is between 21.0 and 23.0 °C with an airflow velocity of 0.15 m/s [6].

An index called the predicted mean vote (PMV) was proposed by Fanger [7] to predict the average vote of a large group of people on the thermal sensation scale. It depends on six factors: metabolic rate, clothing insulation, air temperature, humidity, air velocity, and

* Corresponding author. Tel.: +39 (0) 935536448; fax: +39 (0) 935 536951.
E-mail addresses: antonio.messineo@unikore.it, messineo.ingegneria@gmail.com (A. Messineo).

[1] Typically, the standard for thermal comfort is defined by the operative temperature, which is the average of the dry-bulb air temperature and the mean radiant temperature at a given place in a room.

0360-1323/$ – see front matter © 2013 Elsevier Ltd. All rights reserved.
http://dx.doi.org/10.1016/j.buildenv.2013.10.020

mean radiant temperature. The PMV represents a subjective quantification of the comfort sensation of the occupants in indoor environments. Other variations of the PMV, e.g., the PMV_{NV} [8] and the PMV(SET*) [9], have also been developed. These variations are more appropriate for situations in which only natural ventilation (no air conditioning) is used.

The utilization of conventional approaches to assure indoor thermal comfort in buildings (e.g., on-off devices and timers with set temperatures, which do not vary dynamically with the temperature in the monitored thermal zone) causes significant energy consumption. Liu et al. [10] and Stoops [11] showed that guaranteeing thermal comfort can lead to high energy consumption, especially if an optimal combination of the various influential variables (i.e., air temperature, air velocity, air humidity and radiant temperature) is not achieved. In contrast, they demonstrated that extreme energy saving measures can act to the detriment of the thermal comfort, causing negative effects on human health.

Therefore, a correct identification of the relationship between environmental parameters and energy requirements linked to thermal comfort preservation is extremely important. Weather conditions certainly have an influence on this relationship [12–14]. However, they are not the only influential elements because internal heat gains, thermal insulation, natural ventilation, air infiltration and behavior of the occupants also play an important role, especially in hot and humid climates [15]. Not surprisingly, in terms of electricity consumption, total building energy consumption over the last few years was second only to the industrial sector in Sicily (Italy) [14], with industrial activities having high refrigeration needs playing an important role [16,17]. Moreover, in densely built areas, the high energy consumption of summer air conditioning and the consequential emissions to the atmosphere are certainly enhanced by the well-known urban heat island (UHI) phenomenon [18–20], which increases building cooling loads (especially during peak hours) and reduces the efficiency of air conditioning appliances [21]. Furthermore, the UHI also enhances the heat release during night hours (due to the high thermal inertia of construction materials), thus further increasing the required energy demand for cooling. It is therefore apparent that an appropriate temperature and humidity control strategy is important to improve the energy efficiency of a building-HVAC integrated system, still guaranteeing thermal comfort conditions for building occupants [22].

In this paper, the effect of air temperature and other weather parameters (e.g., relative humidity and wind speed) are considered to train a neural network model aimed at forecasting indoor temperature to feed a fuzzy controller, which has the ultimate goal of keeping acceptable indoor conditions from the thermal comfort point of view.

The main goal of this paper is to show the design of a suitable neural temperature predictor (especially concerning the *order* selection of the regressor) and present the overall architecture of the coupled neuro-fuzzy model.

2. State of the art

A large number of studies exist regarding assessing, creating and maintaining indoor comfort conditions for building occupants [23]. In addition to parameters including thermal–physical properties of building materials and architectural features of the building (e.g., orientation, layout, transparency ratio, and shape factor), satisfaction with the indoor environmental quality (IEQ) is influenced by individual characteristics and by physiological parameters, e.g., age, clothing and physical activity [24].

Several scientific papers have applied soft computing and machine learning techniques to weather parameter forecasts; some applications of fuzzy logic controllers (FLCs) of indoor thermal parameters also exist [25–28]. For example, a fuzzy proportional integral derivative (PID) controller was proposed by Calvino et al. [27] for the microclimate control of confined indoor environments. The PMV [4] was assumed to be the driving index for the control procedure. In Refs. [25], "comfort" was represented by a 3D fuzzy set in a fuzzy cube. The authors presented the structure of an FLC and proposed its parameters be tuned using genetic algorithms. The proposed system was able to successfully manage thermal and visual comfort, air quality and energy savings in an office building.

Furthermore, artificial neural networks (ANNs) have been widely used to forecast indoor and outdoor air temperature in building applications, sometimes coupled with fuzzy logic (FL) systems [29]. However, an extensive literature on the coupling of neural and fuzzy models for comfort evaluation is missing.

Mustafaraj et al. [30] compared an auto-regressive model with external inputs (ARX) and its neural network-based nonlinear counterpart (neural network auto-regressive with external inputs – NNARX) to forecast the thermal behavior of an office located in a modern building using internal and external weather data to forecast the dry bulb temperature and the relative humidity of the room at different time horizons (from 30 min to 3 h ahead). Both models yielded acceptable forecasts. However, the NNARX model outperformed the ARX because temperature and relative humidity are governed by nonlinear diffusion equations and the linear models are not capable of capturing the (nonlinear) system dynamics.

Soleimani-Mohseni et al. [31] applied an ANN model (a feed-forward multi-layer perceptron – MLP – trained using the Levenberg–Marquardt algorithm) and an ARX model to estimate the operative temperature in buildings. They similarly concluded that the nonlinear ANN model outperformed the linear ARX model.

Huang et al. [32] used a multiple-inputs, multiple-outputs (MIMO) ANN model (trained with Bayesian regulation to obtain the optimal regularization parameters) for the prediction of the zone temperature in a building. The model proved to be able to capture fairly well the intrinsic dynamics of the investigated system. Trained with data sampled on a 10-min time step, the model yielded mean square errors (MSEs) ranging from 0.118 °C to 0.258 °C and mean absolute errors (MAEs) ranging from 0.211 °C to 0.422 °C for a 2-days-ahead forecast.

Thomas and Soleimani-Mohseni [33] compared first and second order ARX and ARMAX models for two-steps-ahead[2] indoor temperature forecast with an auto-regressing moving average with external inputs (ARMAX) models and Box-Jenkin (BJ) models. They concluded that the BJ and ARMAX models gave nearly the same MSE and MAE values for test data as the ARX models when using models of the same order. However, the NNARX models always outperformed (in terms of the MAE) the ARX models.

Mechaqrane and Zouak [34] also presented a comparison between NNARX and ARX models used to predict the indoor temperature of a residential building. The NNARX model performance was significantly better than the ARX model.

Gouda et al. [35] applied a feed-forward MLP trained with the Levenberg–Marquardt algorithm to model the thermal dynamics of building space and heating system to predict indoor temperature 2 h ahead. They used singular value decomposition (SVD) to select the order of the predictor.

Argiriou et al. [36] developed an ANN controller consisting of a meteorological module, which forecasts the ambient temperature and solar irradiance, a heating energy switch predictor module and a module for indoor temperature definition. The controller was

[2] A two-steps-ahead prediction means 30 min ahead, since the sampling interval was 15 min.

designed for solar buildings, i.e., for buildings that have large southward oriented openings and a significant thermal mass.

In Ref. [37], MLP ensembles were applied to model the nonlinear relationships between energy consumption, control settings (supply air temperature and supply air static pressure), and a set of uncontrollable parameters for minimizing the energy to air condition a typical office-type facility. They were compared with other data-driven algorithms (e.g., chi-squared automatic interaction detector – CHAID, classification and regression tree – C&RT – algorithm, support vector machine – SVM, multi-layer perceptron – MLP, boosting tree, random forest, and multivariate adaptive regression spline – MARSpline). The MLP ensembles were proven to outperform the other algorithms.

In Ref. [38], the energy consumption of an HVAC system was optimized using a dynamic ANN. The minimization of the energy consumed while maintaining the indoor room temperature at an acceptable level was accomplished with bi-objective optimization. The model was solved with three variants of the multi-objective particle swarm optimization algorithm.

In addition to using the approaches to regulate the comfort levels based on controlling measured parameters, several building optimization applications make use of computer models of the building-plant system and its interaction with the external environment (i.e., weather variables and airflows). The computer models allow simulated values of comfort indicators for formulating optimization problems without the need for measurements.

For example, in Ref. [39], the building simulation software ESP-r was used to generate a database of end-of-thermostat setback (EoS) values for two office buildings using climate records in Kuwait. The EoS data were used for training and testing general regression neural network (GRNN) models aimed at optimizing air conditioning setback scheduling in which the designated temperature inside the building was restored in time for the start of business hours.

In Ref. [40], the airflow in and around a building is simulated using a computational fluid dynamics (CFD) model. The produced airflow patterns are utilized to predict thermal comfort indices, i.e., the PMV and its modifications for non-air-conditioned buildings, with respect to various occupant activities. Mean values of these indices within the occupied zone are calculated for different window-to-door configurations and building directions to generate a database of input–output data pairs used to train and validate radial basis function (RBF) ANN input–output "meta-models". In Ref. [41], the same modeling strategy was used. However, indoor air quality indices, e.g., ventilation effectiveness based on carbon dioxide and volatile organic compound (VOC) removal were also included as output (objective) variables in addition to the PMV index.

In Ref. [42], a hybrid model for effectively controlling indoor thermal comfort in an HVAC system was presented. The first part of the model is related to the building structure; the second part is a fuzzy model associated with the indoor thermal comfort itself. To evaluate indoor thermal comfort situations, the PMV and percentage of dissatisfaction (PPD) indicators were used.

3. Materials and methods

In this paper, only outdoor temperature, air relative humidity, wind speed and indoor temperature recorded in previous time steps were used as regressors to perform the indoor temperature forecast and thereby drive the controller. In fact, in its current state, the fuzzy controller is only driven by the indoor temperature forecasted by the NNARX module; no variation of heat gains, physiological parameters and individual characteristics of the occupants (e.g., age, clothing, and activity) were considered for driving the controller. Including these other parameters would certainly provide a more realistic description of the physical system. However, these parameters are not yet included in this preliminary model setup. Comfort temperature (both for the winter and the summer scenario) in the studied environment is considered as a temperature falling within the acceptability range proposed by ASHRAE [4]. The proposed model has a cascade structure in which the nonlinear indoor temperature forecasting module (in a NNARX module) is directly linked to the FLC module, which acts on the HVAC system (on/off actions and regulation of the inlet air speed).

3.1. NNARX temperature forecast model

The input parameters of the NNARX model are the dry bulb outdoor air temperature (T_a), relative humidity (RH), wind speed (WS) and dry bulb indoor air temperature (T_i) from the preceding time steps.

The NNARX model computes the expected indoor temperature at time k one step ahead (at time $k-1$). The difference ΔT between the temperature at time k and the temperature at time $k-1$ allows the FLC to run the fan coils to tune the inlet air speed.

The predictor associated with the NNARX model is of the form [43]

$$\widehat{y}(t|\theta) = \widehat{y}(t|t-1,\theta) = g(\varphi(t),\theta), \tag{1}$$

where $\widehat{y}(t)$ is the value of y at time t predicted by the model, θ is a vector containing the weights of the NN, g is the function realized by the NN and $\varphi(t)$ is a vector containing the regressors, given by

$$\varphi(t) = [y(t-1)\ldots y(t-n_a)u(t-n_k)\ldots u(t-n_b-n_k+1)]^T. \tag{2}$$

Here, u refers to the set of inputs and n_a, n_b and n_k are the parameters defining the *order* of the regressors.

To select the number of past signals used as regressors, i.e., the *model order*, the differential entropy-based method proposed in Ref. [44] and implemented in the related Matlab toolbox [45] is applied in this study. More details on the method are contained in the Appendix.

In the case study used in the present work, this method is applied to estimate the embedding parameters for the NNARX model external inputs, i.e., WS (m/s), RU (%) and T_a (°C), and forecast the indoor air temperature in an office room located in the town of Enna (Italy) at different intervals ahead of time. All time series used for the network training have a sampling step of 1 h. The weather data are recorded by a weather station located on the roof of the building and the indoor temperatures are collected using an Onset Hobo-U10 data logger fixed at a height of 1.8 m from the floor on a pedestal approximately located at the center of the room.

Fig. 1 shows a cross section of the building and picture of the pedestal with the temperature sensor installed.

The data are divided into two sets to simulate two different scenarios: one for summer (from June to August) and the other for winter (from November to February) situations.

The NNARX models are tested with a number of neurons in the hidden layer, varying from 10 to 70 (with an increase of 10 neurons for each test). They are trained using the Levenberg–Marquardt algorithm [46] with the following training parameters (see Ref. [47] for further details):

- Performance goal = $5\cdot10^{-3}$
- Learning rate = 0.1
- Maximum failure number for validation = 20
- Marquardt adjustment parameter = 0.05

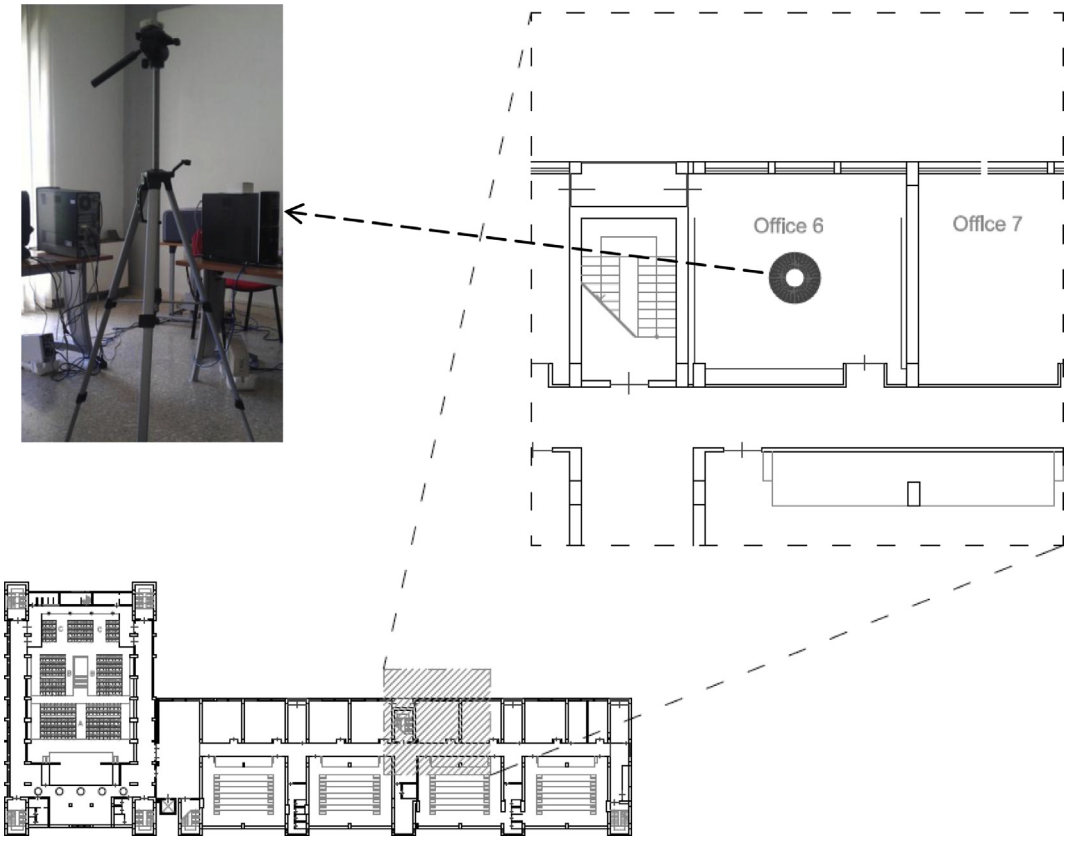

Fig. 1. Cross section of the building with a magnification on the location of the office room equipped with the temperature sensor. The top left part of the picture shows a detail of the pedestal with the sensor (Onset Hobo-U10 data logger), which is located in the point marked with the hollow circle.

For each parameter, the differential entropy based method is used with a number of surrogates ($N_s = 5$). Furthermore, to monitor the robustness of the method, the time series are resampled at different rates, spanning from 1 to 5.

Figs. 2–5 show the surfaces of the entropy ratio (ER) function (see the Appendix) obtained for T_a, T_i, RU and WS in the winter and summer scenarios. The surface minimums are marked with a red circle; the corresponding optimal values selected for the embedding parameters are marked on the picture.

In Table 1, the selected values of the embedding dimension[3] (m_{opt}) and the delay time (τ_{opt}) for both the summer and winter cases are shown for all the regressors.

The vector $\varphi(t)$, given by

$$\varphi(t) = [T_a(t-3)\ldots T_a(t-12), T_i(t-3)\ldots T_i(t-15), \mathrm{RU}(t-3)\ldots\mathrm{RU}(t-27), \mathrm{WS}(t-6)\ldots\mathrm{WS}(t-42)]^T, \quad (3)$$

$$\varphi(t) = [T_a(t-1)\ldots T_a(t-5), T_i(t-1)\ldots T_i(t-5), \mathrm{RU}(t-3)\ldots\mathrm{RU}(t-24), \mathrm{WS}(t-9)\ldots\mathrm{WS}(t-81)]^T, \quad (4)$$

contain the regressors corresponding to the NNARX model used for the winter and summer cases, respectively.

The output of both models is the temperature $T_i(t)$.

[3] m_{opt} and τ_{opt} represent the optimal values of the parameters m and τ defined in the Appendix.

Fig. 6 shows the structure of the NNARX models used for the winter and the summer scenarios.

To guarantee good general model performance (i.e., the capacity of providing good estimates on unknown data samples) and prevent the risk of *over-fitting* the training data, the *early stopping* technique was used. In early stopping, the entire dataset is split into three subsets: a training set, a validation set and a test set. The training dataset is used for computing the gradient of the cost function (which is a function of the MSE) and updating the network weights. The error on the validation set is monitored during the training process. During the initial phase of training, both the validation error and the training set error typically decrease. However, when the network begins to over-fit the data, the error on the validation set typically begins to rise. When the validation error increases for a specified number of iterations, the training is stopped and the network's weights at the minimum of the validation error are returned.

In our case, the training set comprised 70% of the data; 15% of the data are used for the validation set and 15% are retained for the test set. The data are normalized between 0 and 1 using min–max normalization before feeding the neural network.

The validation performance and training state of the networks are given in Figs. 7 and 8.

During the training, the maximum failure number for validation is set to 20, which means the training stops when the validation error continuously increases for 20 iterations starting from the best validation performance, i.e., the MSE minimum.

The forecasting performances of the networks are assessed using the test set data and against the error measures presented in Table 2 where Y_i is the value of the i-th actual observation, $\hat{Y}_i$ is its

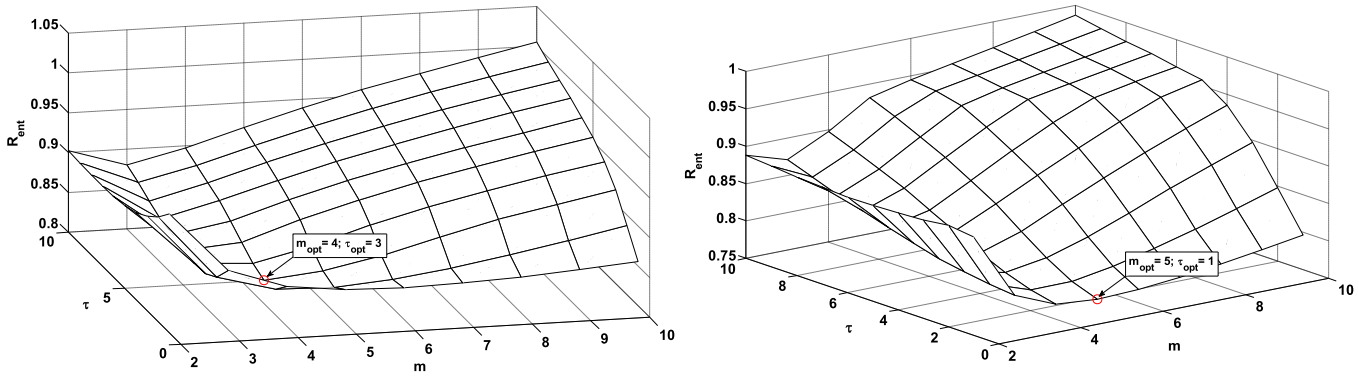

Fig. 2. ER surface for the variable T_a in winter scenario (left hand side) and summer scenario (right hand side).

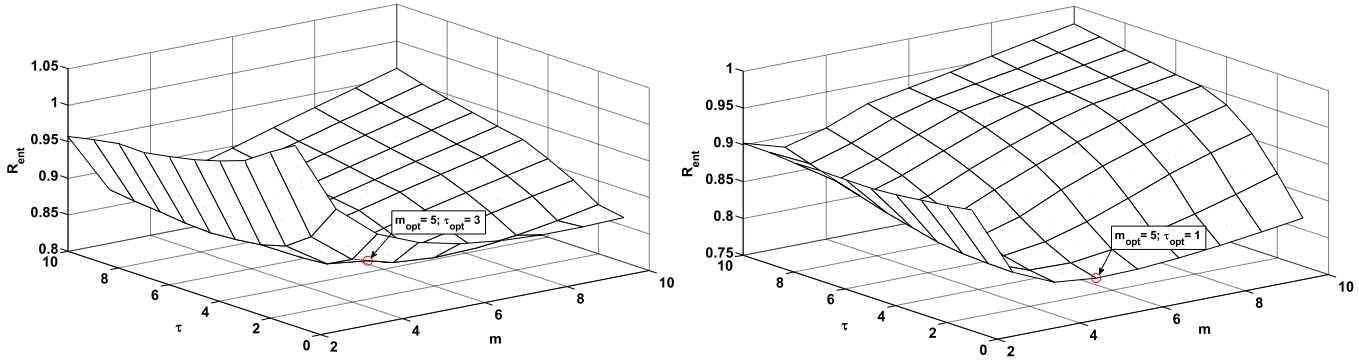

Fig. 3. ER surface for the variable T_i in winter scenario (left hand side) and summer scenario (right hand side).

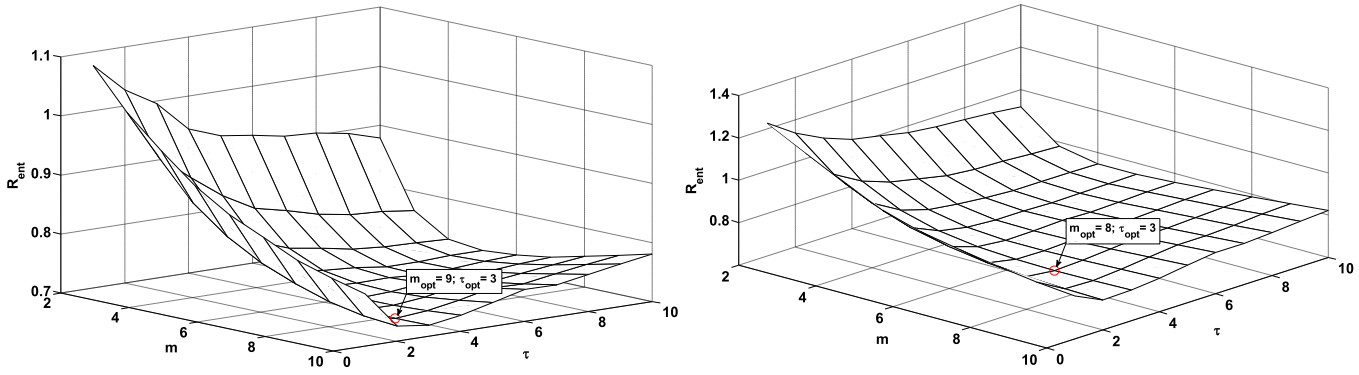

Fig. 4. ER surface for the variable RU in winter scenario (left hand side) and summer scenario (right hand side).

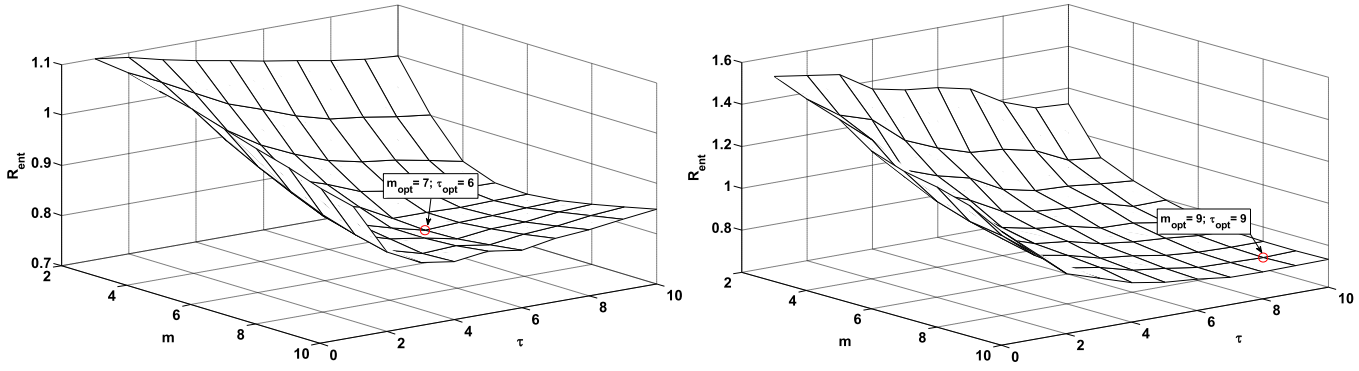

Fig. 5. ER surface for the variable WS in winter scenario (left hand side) and summer scenario (right hand side).

Table 1
Selected (optimal) values of the embedding parameters used for the NNARX model.

	Regressors (Winter scenario)				Regressors (Summer scenario)			
	T_a	T_i	RH	WS	T_a	T_i	RH	WS
m_{opt}	4	5	9	7	5	5	8	9
τ_{opt}	3	3	3	6	1	1	3	9

T_a = outdoor air temperature; T_i = indoor air temperature; RU = outdoor relative air humidity; WS = wind speed.

forecasted value, $\overline{\widehat{Y}}$ is the mean of the predicted values on the test dataset, $\overline{Y}$ is the mean value of the test dataset, $e_i = Y_i - \widehat{Y}_i$ is the forecast error, $q_i = \frac{e_i}{\frac{1}{N_t-1}\sum_{i=2}^{N_t}|Y_i - Y_{i-1}|}$ (in which N_t is the total number of observations in the test set) is the scaled error, $p_i = \frac{Y_i - \widehat{Y}_i}{Y_i} \cdot 100$ is the absolute percentage error, σ_{pred} is the standard deviation of the predictions obtained on the test set data and σ_{test} is the standard deviation of the test set data.

As explained in Section 4, on the basis of the forecast performances, the chosen networks are those with 30 neurons in the hidden layer for the winter scenario and 10 neurons in the hidden layer for the summer scenario.

3.2. Combined fuzzy logic controller (FLC) and NNARX model application

In the application shown in this paper, the FLC acts on the indoor thermal comfort conditions to always maintain the temperature within the range recommended by ASHRAE [4,5]. Fuzzy controllers coupled with HVAC systems have the advantage of being characterized using linguistic rules instead of complex analytical expressions [26]. In this paper, we show a simulated scenario of a typical indoor environmental situation to demonstrate the advantages of using ANN-forecasted parameters as input for an FLC. Only the indoor temperature is used. However, other parameters, e.g., the PMV or the indoor concentration of carbon dioxide, could be used when data are available. The FLC, which runs the HVAC plant, is activated by the difference ΔT between the value $T_i(k)$ of the predicted indoor temperature at time k (one hour ahead) and the value $T_i(k\text{-}n)$ of the indoor temperature measured at time $(k\text{-}n)$, where n = 60, 55,…, 5 min. In our experiments, we simulated the switching on or off of the HVAC system and the regulation of the inlet air speed (here called ON/OFF speed) by the FLC.

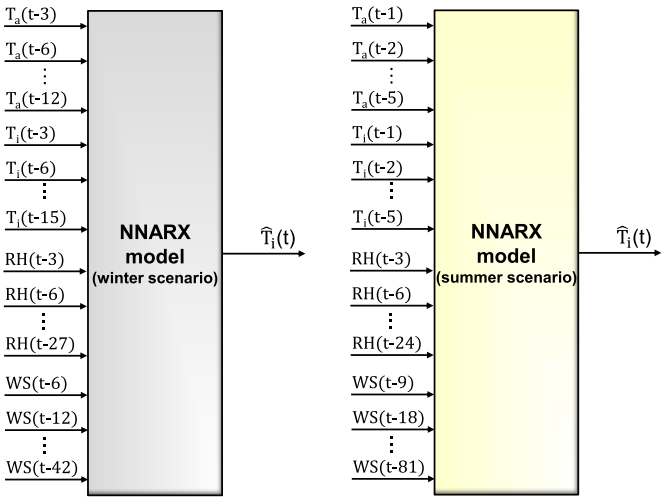

Fig. 6. Structure of the NNARX models used in the case study for the winter (left hand side) and summer (right hand side) scenarios.

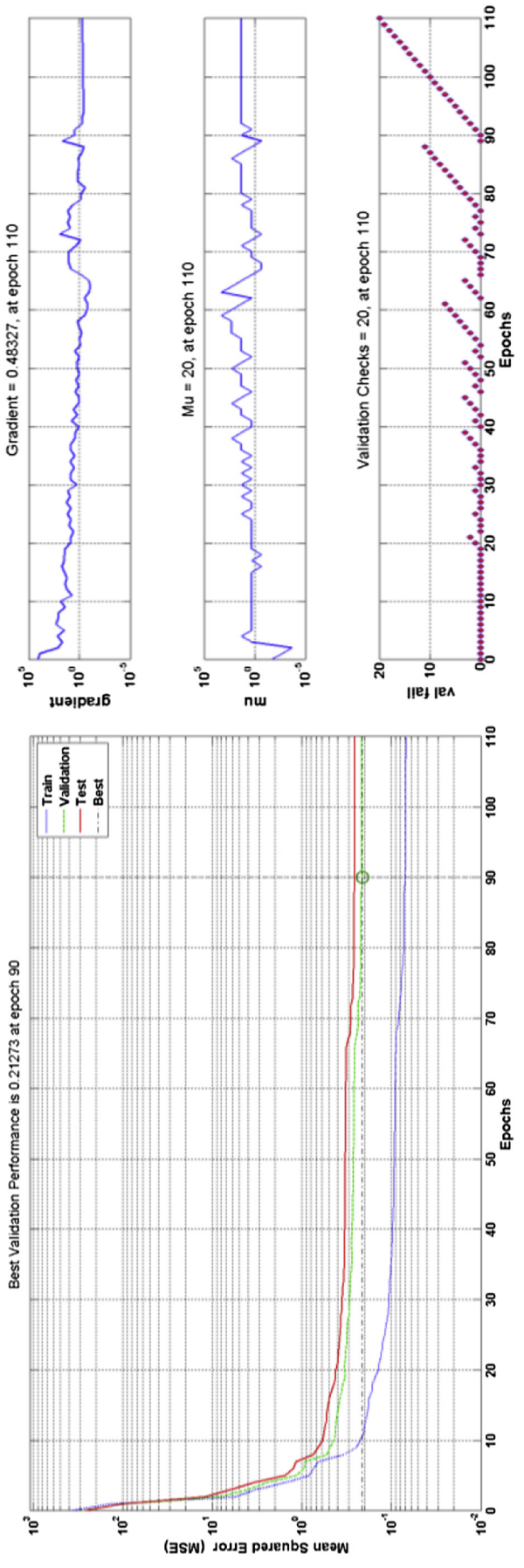

Fig. 7. Best validation performance (MSE) (left hand side) and training state (right hand side) for the NNARX used for the winter scenario. Note: mu = Marquardt adjustment parameter; val fail = number of iterations for which the validation error continuously increased after the last decrease.

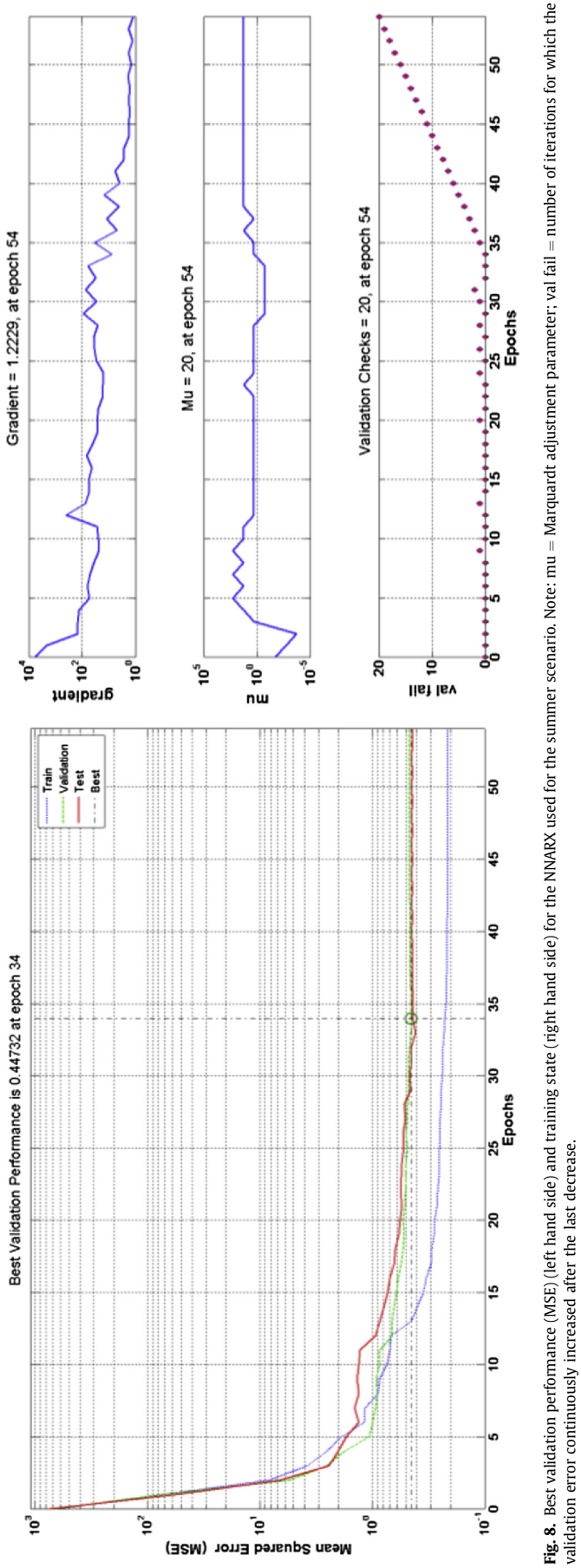

Fig. 8. Best validation performance (MSE) (left hand side) and training state (right hand side) for the NNARX used for the summer scenario. Note: mu = Marquardt adjustment parameter; val fail = number of iterations for which the validation error continuously increased after the last decrease.

Internal heat gains are not directly considered. This is certainly a limitation of the model, which, to be fully operational, will need on one hand a proper consideration of the heat gains in the input signal and on the other hand to base the control signal for the HVAC not only on the indoor air temperature, considering that the air temperature does not fully represent the thermal comfort/discomfort sensation, but just one of the factors affecting it. In the current status of the model, heat gains are only indirectly considered through their effect on the variation of the indoor temperature, which is recorded by the data logger.

In Fig. 9 the adopted control system is schematized.

The controller is fed with the crisp numerical values of $T_i(k)$ and ΔT_i, which are converted into linguistic values using a chosen set of membership functions.

Five linguistic values are used:

- Very Hot (VH);
- Slightly Hot (SH);
- Comfort (COM);
- Slightly Cold (SC);
- Very Cold (VC).

In Tables 3–5, the membership functions used for T_i in the summer and winter scenarios and for the difference ΔT_i, respectively, are shown. They are graphically represented in Figs. 10–12, respectively.

The controller has the task of elaborating these linguistic values using an inference mechanism based on a set of if-then rules. These are later combined in the FLC, which produces a membership function that can be represented by various functional shapes (e.g., Gaussian, triangular, trapezoidal, and cosine). It is then possible to determine the linguistic output (the fuzzy conclusion), which can assume one of the above presented values. The inference mechanism thus determines the correct output according to the fuzzy inference rules presented in Table 6.

For example, if one is dealing with the summer scenario and the predicted value for $T_i(k)$ is 26 °C, the fuzzy value becomes SH and if $\Delta T_i = -2$ °C, the fuzzy value becomes SC. Thus, the inference value is COM. Afterward, the FLC defuzzifies this value, converting it to crisp logic decisions suitable to drive the HVAC system. The defuzzification process was carried out using Mizumoto's functions centroid and maximum [48].

The regulation of the inlet air speed in the HVAC system is based on triangular Mamdani functions [49]. The Mamdami model is a crisp model of a system, i.e., it takes crisp inputs and produces crisp outputs. This operation is performed on the basis of user-defined fuzzy rules on user-defined fuzzy variables.

The operation of the Mamdani rule base can be decomposed into four parts: 1) mapping each of the crisp inputs into a fuzzy variable (fuzzification), 2) determining the output of each rule given its fuzzy antecedents, 3) determining the aggregate output(s) of all fuzzy rules, and 4) mapping the fuzzy output(s) to crisp output(s) (defuzzification).

4. Results and discussion

4.1. NNARX model

In this section, the results obtained with the NNARX model on the test set data are presented for both the winter and summer scenarios. Table 7 shows the values attained for the performance measures for the NNARX used in the winter scenario. Table 8 shows the analogous values for the NNARX model used in the summer scenario.

The values in bold in Tables 7 and 8 are the best attained using the performance measures for all the trained networks. From these

Table 2
Error measures used to assess the forecasting performances of the NNARX models.

Error measure	Formula
Mean Squared Error (MSE)	$\text{mean}(e_i^2)$
Root Square Mean Error (RMSE)	$\sqrt{\text{MSE}}$
Mean Absolute Error (MAE)	$\text{mean}(\lvert e_i\rvert)$
Median Absolute Error (MdAE)	$\text{median}(\lvert e_i\rvert)$
Mean Absolute Scaled Error (MASE)	$\text{mean}(\lvert q_i\rvert)$
Mean Absolute Percentage Error (MAPE)	$\text{mean}(\lvert p_i\rvert)$
Normalized Mean Absolute Percentage Error (NMAPE)	$\frac{1}{N_t}\sum_{i=1}^{N_t}\frac{\lvert Y_i-\widehat{Y}_i\rvert}{\max_{i=1}^{N_t}(Y_i)}\cdot 100$
Median Absolute Percentage Error (MdAPE)	$\text{median}(\lvert p_i\rvert)$
Symmetric Mean Absolute Percentage Error (sMAPE)	$\frac{1}{N_t}\sum_{i=1}^{N_t}\frac{\lvert Y_i-\widehat{Y}_i\rvert}{(\lvert Y_i\rvert+\lvert\widehat{Y}_i\rvert)/2}\times 100$
Coefficient of correlation (R_0)	$\frac{1}{N_t\sigma_{pred}\sigma_{test}}\sum_{i=1}^{N_t}(\widehat{Y}_i-\overline{\widehat{Y}})(Y_i-\overline{Y})$

performances measures, we decided to choose the networks with 30 neurons and 10 neurons in the hidden layer for the winter and summer scenarios, respectively (the corresponding columns in Tables 7 and 8 are highlighted with a gray background).

Fig. 13 shows the values of the measured (test set data) and forecasted indoor temperature (as well as the corresponding forecasting error) for the winter scenario. Fig. 14 refers to the summer scenario. In both cases, the temperatures are those recorded when the HVAC system is not functioning, i.e., they refer to the building envelope in natural evolution dynamics.

4.2. Simulation of the coupled NNARX-FLC system

The last phase of the study consisted of the FLC simulation, which, based on the indoor temperature values forecasted by the NNARX model and on the temperature detected in the room by the data logger (recorded every 5 min), dynamically determines the ON/OFF time and the inlet air speed of the HVAC system. The time step between two consecutive regulation signals sent by the controller to the HVAC system was set to 5 min, i.e., equal to the sampling interval of the indoor temperature data logger.

Table 3
Membership function T_i used for the summer scenario.

Linguistic values	$T_i(k)$ [°C] interval
VH	29 ÷ 38
SH	25 ÷ 28
COM	24.5 ÷ 24.5
SC	20 ÷ 24
VC	18 ÷ 19

Table 4
Membership function T_i used for the winter scenario.

Linguistic values	$T_i(k)$ [°C] interval
VH	26 ÷ 27
SH	23 ÷ 25
COM	22 ÷ 22
SC	19 ÷ 21
VC	9 ÷ 18

Table 5
Membership function ΔT_i.

Linguistic values	ΔT_i [°C] interval
VH	3 ÷ 9
SH	1 ÷ 3
COM	0 ÷ 0
SC	−1 ÷ −3
VC	−3 ÷ −9

Figs. 15 and 16 refer to the application of the controller in the winter and summer situations, respectively. The evolution of the inlet air speed injected by the fan coils and the indoor air temperature forecasted by the NNARX model are plotted as a function of time during a typical day. The inlet air speed was set to an initial value of 2 m/s. When the NNARX model forecasts a temperature

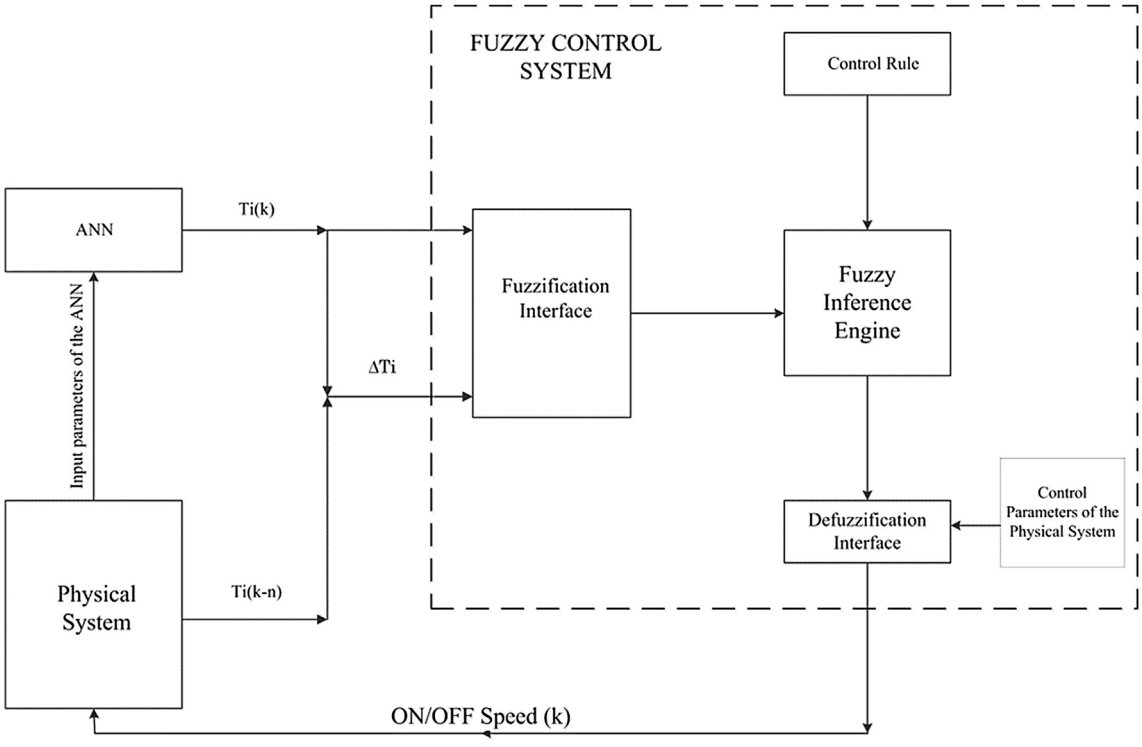

Fig. 9. Simplified scheme of the coupled ANN-FLC system for temperature control.

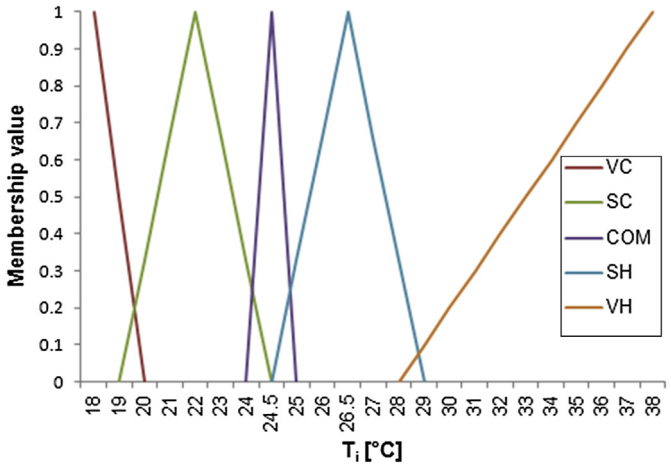

Fig. 10. Membership functions T_i (summer).

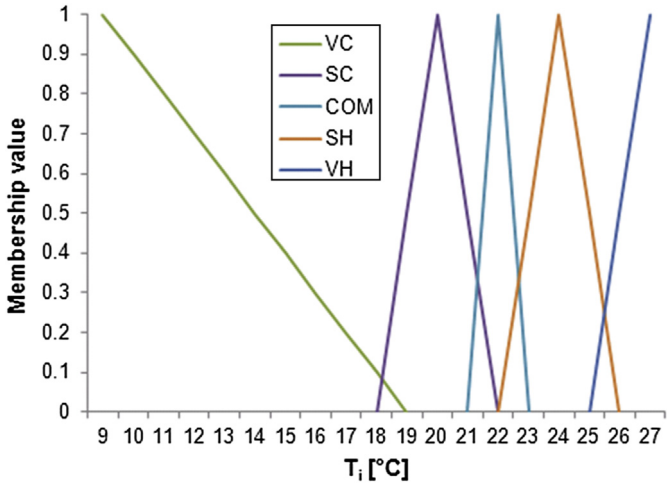

Fig. 11. Membership functions T_i (winter).

that would fall outside the comfort range, the controller drives the HVAC system accordingly to adjust the indoor temperature in the correct direction. As mentioned above, in our test, the minimum time lag between two subsequent variations of the inlet air speed

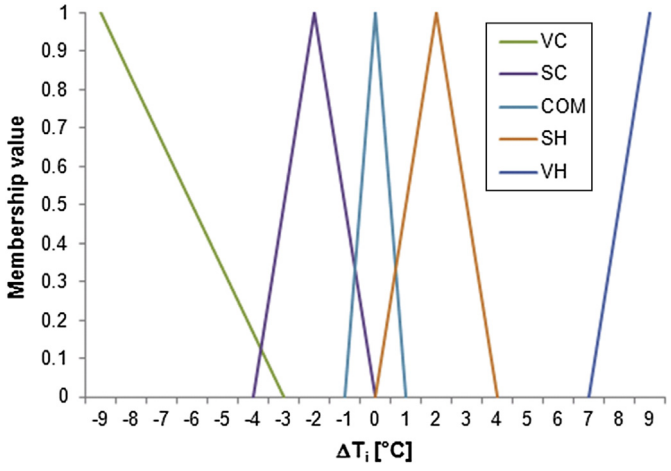

Fig. 12. Membership function ΔT_i.

Table 6
Fuzzy inference rules of FLC.

ON/OFF speed		$T_i(k)$				
		VC	SC	COM	SH	VH
$\Delta T_i(k)$	VC	VH	VH	VH	SH	SH
	SC	VH	SH	SH	COM	COM
	COM	SH	COM	COM	COM	SC
	SH	COM	COM	SC	SC	VC
	VH	SC	SC	VC	VC	VC

Table 7
Performance measures and number of training epochs for each of the seven NNARX models trained in the winter scenario.

Neurons in the hidden layer	*10*	*20*	*30*	*40*	*50*	*60*	*70*
Training epochs	*313*	*133*	*31*	*84*	*21*	*77*	*103*
MSE	**0.217**	0.244	0.260	0.509	0.462	0.365	0.391
RMSE	**0.466**	0.494	0.510	0.714	0.679	0.604	0.626
MAE	0.340	0.373	**0.250**	0.463	0.580	0.512	0.589
MdAE	0.204	0.270	**0.167**	0.343	0.441	0.394	0.421
MASE	0.751	0.823	**0.553**	1.022	1.282	1.131	1.189
NMAPE	**1.323**	1.581	2.280	2.153	2.699	2.382	2.505
MAPE	4.749	5.246	**3.583**	6.802	8.068	6.876	8.219
MdAPE	2.234	2.986	**1.709**	3.532	4.683	4.232	4.259
sMdAPE	2.246	2.982	1.696	3.534	4.628	4.233	4.261
R_0	0.990	0.981	0.990	0.980	0.982	**0.991**	0.987

injected by the fan coils (if necessary) is 5 min, which is the sampling step of our indoor temperature measurements.

In practice, the NNARX model learns to tune the fuzzy control off-line. Thereafter, the FLC uses the trained ANN on-line to optimize the control. The goal of this on-line dynamic control of the inlet air speed based on an expected (forecasted) temperature rather than just on the actual temperature measured in the room is to provide a better adaptation of the HVAC plant to the intrinsic dynamics of the nonlinear system that governs the temperature evolution. The underlying mechanisms determining temperature evolution with time are learned by the ANN model based on the intrinsic relationship existing between its inputs and output (the forecasted indoor temperature). The knowledge extracted by the ANN is then transmitted on-line to the FLC, thus preventing unnecessary energy consumption due to non-optimal regulation of the inlet air.

This preliminary model setup carries several limitations. First, because the control mechanism is triggered only by the variation of the indoor temperature, other important contributors to the comfort sensation (e.g., visual comfort, indoor air quality, and

Table 8
Performance measures and number of training epochs for each of the seven NNARX models trained in the summer scenario.

Neurons in the hidden layer	*10*	*20*	*30*	*40*	*50*	*60*	*70*
Training epochs	*68*	*27*	*21*	*28*	*17*	*15*	*21*
MSE	**0.333**	0.664	0.424	0.574	0.652	0.596	0.482
RMSE	**0.577**	0.815	0.652	0.758	0.807	0.772	0.694
MAE	**0.289**	0.664	0.424	0.574	0.552	0.657	0.482
MdAE	0.356	0.390	0.524	0.426	0.469	0.589	**0.211**
MASE	**0.607**	0.727	0.888	0.711	0.759	0.903	0.948
NMAPE	**1.195**	1.430	1.747	1.398	1.493	1.775	1.864
MAPE	**1.745**	2.097	2.554	2.021	2.185	2.587	2.706
MdAPE	**1.330**	1.472	1.986	1.635	1.774	2.265	2.106
sMdAPE	**1.331**	1.475	1.974	1.622	1.763	2.244	2.119
R0	**0.984**	0.969	0.979	0.972	0.967	0.972	0.979

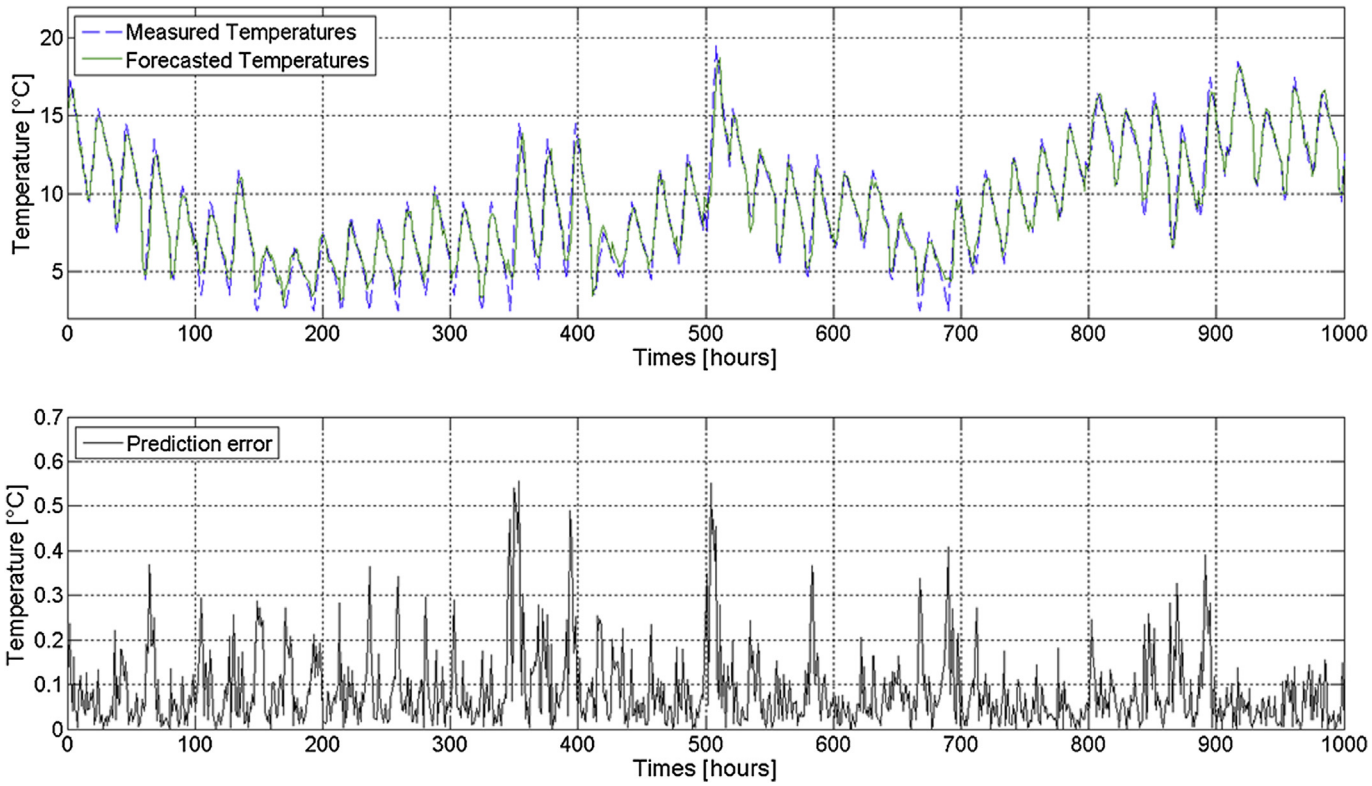

Fig. 13. Measured and forecasted indoor temperatures for the winter scenario (NNARX with 30 hidden neurons).

variables concurring to the calculation of PMV) are disregarded. Furthermore, only a representative temperature measured at a single point location within the room was considered. This fact clearly does not allow the model to consider local discomfort due to temperature non-uniformity in the room (e.g., high radiant temperature asymmetry or too low or too high internal surface temperatures) and head to ankle temperature differences.

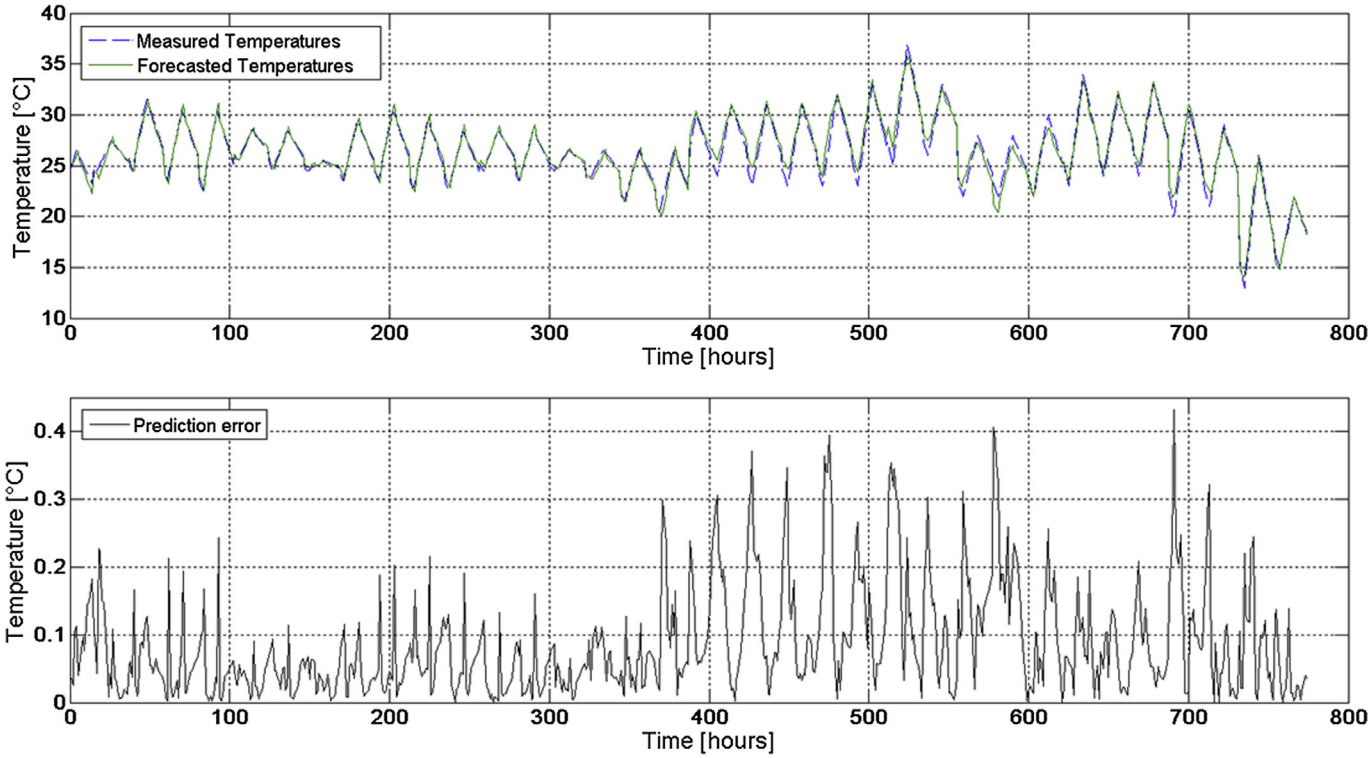

Fig. 14. Measured and forecasted indoor temperatures for the summer scenario (NNARX with 10 hidden neurons).

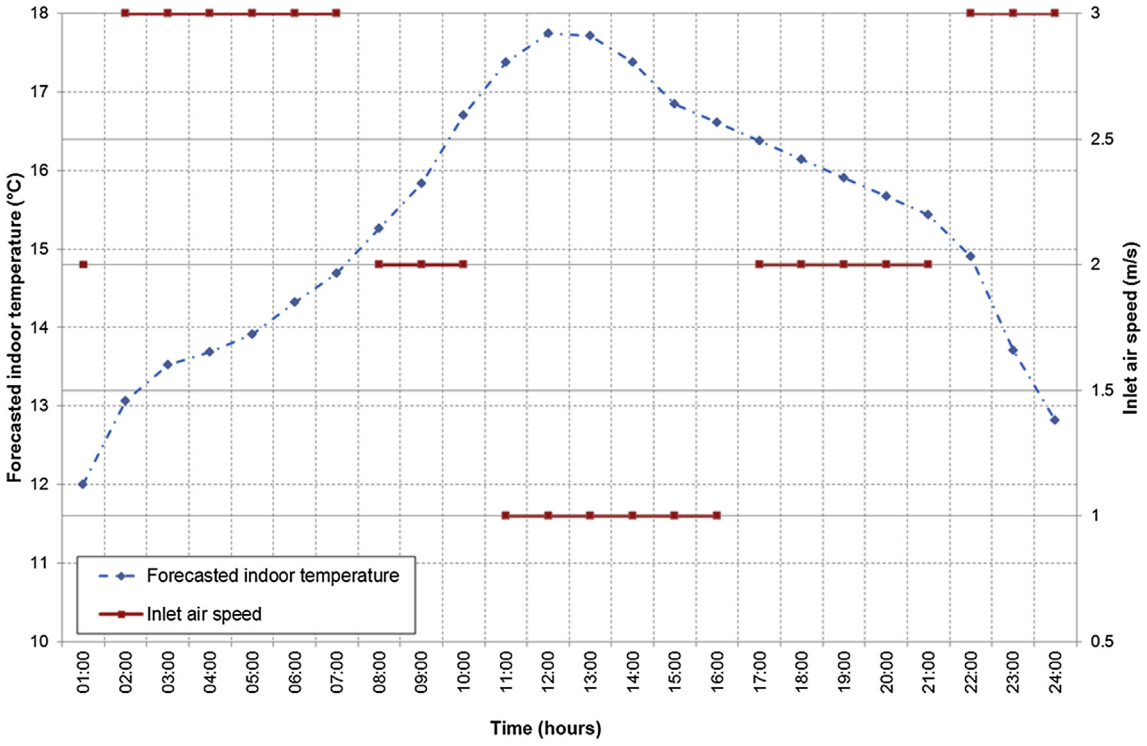

Fig. 15. ON/OFF speed of the HVAC system as a function of the indoor temperature (winter case).

Another aspect of the current model settings that from some points of view may be seen as a limitation is the fact that it is trained with measured data (i.e., both indoor temperature and weather parameters) and therefore is representative of the intrinsic dynamics only of the system (building) it was built on. To be completely transferable to other buildings, a computer model of the building-plant system (e.g., created with thermal building simulation software) should have been used so that the variation of

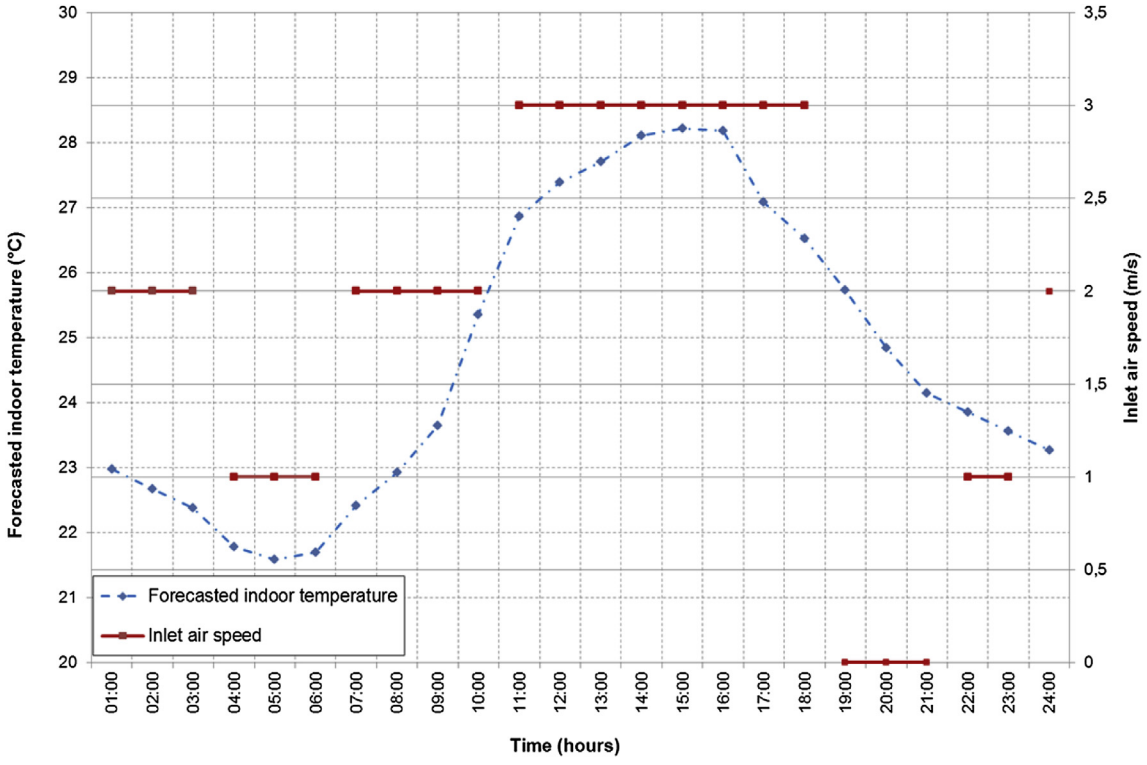

Fig. 16. ON/OFF speed of the HVAC system as a function of the indoor temperature (summer case).

parameters (e.g., building orientation, construction materials, occupation rate, and internal heat gains) in the computer model would be adapted for different physical situations.

Nonetheless, the paper carefully addresses the difficult task of the model order selection in the forecasting module and presents a model setup that lends itself to be made more complex by adding new control variables when new data become available.

5. Conclusions

This paper demonstrates a FLC of indoor temperature fed by an indoor temperature predictor. The temperature prediction is carried out using an NNARX model, which attained good forecasting performances. The actions activated by the controller at a generic time t are thus driven not by the temperature measured at time t but by the temperature forecasted for time $t + 1$. This approach allows for better dynamic control of the ventilation rate to assure constant indoor thermal comfort.

Although the coupling of neural and fuzzy models for the control of environmental parameters to maintain thermal comfort in indoor environments is not novel, this paper provides a particular focus on the optimal selection of the embedding parameters of the NNARX model, which is usually not an easy task in time series prediction problems.

As a result of the efficient dynamical regulation of the on/off times of the HVAC system and its inlet air speed, a more efficient use of energy is expected with respect to simple on–off devices, timers with fixed set point temperature or controllers whose correction actions are based only on the temperature detected in the controlled room rather than on the temperature expected at a future time.

The positive effect (maintenance of thermal comfort conditions in the indoor environment) of the temperature regulation provided by the coupling of an NNARX indoor temperature forecast model and an FLC are even more important in indoor environments where sudden outdoor temperature spikes occur or where the thermal insulation of the building envelope is poor and therefore significant heat losses occur.

The main goal of this paper was designing a suitable neural predictor of the indoor temperature (especially concerning the *order* selection of the regressor) and presenting the overall architecture of the coupled model, which is to be considered not as a comprehensive one but rather as a preliminary setup. A further application of an improved FLC-based on parameters other than only the indoor temperature (e.g., the PMV and the carbon dioxide concentration) and the comparison of the results with those obtained with a traditional controller is part of a future research plan.

Appendix

The differential entropy-based method is rooted in the *embedding theorem* [50], which guarantees that with a sufficiently long time series $\mathbf{y}(t)$, one can obtain a functional expression f that has a one-to-one correspondence to the original system and recreates its underlying dynamics:

$$\mathbf{v}(t+1) = f[\mathbf{v}(t)], \tag{A1}$$

$$\mathbf{v}(t) = (y(t), y(t+\tau), \ldots, y(t+(m-1)\tau)), \tag{A2}$$

where f denotes the reconstructed dynamical system, $\mathbf{v}$ is the *time delay coordinate vector*, m is the *embedding dimension* and τ is the *delay time*.

The differential entropy method represents any given time series in the so-called "phase space" using a set of delay vectors (DVs):

$$\mathbf{y}(t) = [\mathbf{y}_{t-\tau}, \ldots, \mathbf{y}_{t-m\tau}], \tag{A3}$$

for a given embedding dimension m.

The method is based on the minimization of the following "cost" function which depends on the two embedding parameters m and τ. The main conceptual step is founded in the use of the Kozachenko–Leonenko (K–L) estimate of the differential entropy [51]:

$$H(\mathbf{y}) = \sum_{j=1}^{N} \ln\left(N\rho_j\right) + \ln 2 + C_E, \tag{A4}$$

where N is the number of samples in the dataset, ρ_j is the Euclidean distance of the j-th delay vector to its nearest neighbor, and C_E (≈ 0.5772) is the Euler constant.

However, the K–L entropy estimate given by Eq. (A4) is not robust with respect to dimensionality. This is compensated for by standardizing $H(y,m,\tau)$ with respect to an ensemble of so-called 'surrogates' of signal x [52]. Surrogate data are artificially generated data that mimic some of the properties of the data under study, however not the property for which we are testing for. In the simplest case, N_s surrogates $y_{s,i}$ ($i = 1,\ldots,N_s$) of a signal y are generated by performing a random permutation of the time samples. Using this method, the signal distribution is unaffected and the serial correlations are randomized to obtain a whitened signal with a signal distribution identical to that of the original signal y.

Equation (A4) is used to compute the K-L estimates for the time delay-embedded versions of the original time series $H(y,m,\tau)$ and its surrogates $H(y_{s,i},m,\tau)$ for increasing values of m and τ. The coordinates of the minimum of the "entropy ratio" (ER) yield the optimal embedding parameters:

$$R_{ent}(m,\tau) = \frac{H(y,m,\tau)}{\left\langle H\left(y_{s,i},m,\tau\right)\right\rangle_i} + \frac{m\ln N}{N}, \tag{A5}$$

where $\langle\rangle_i$ denotes the average over i and the second term of the summation is a term accounting for the minimum description length (MDL) [53] of the signal, which allows penalization of higher embedding dimensions and assures that a difference in the K–L estimate (Eq. (A4)) could not be attributed to the number of time samples or DVs.

The surrogate data are generated using the iterative amplitude adjusted Fourier transform (iAAFT) method [54] so that the serial correlations are present in both the original and the surrogate time series, as desired.

References

[1] Chang C, Gershwin ME. Indoor air quality and human health. Clin Rev Allergy Immunol 2004;27(3):219–39.
[2] Thörn A. The sick building syndrome: a diagnostic dilemma. Soc Sci Med 1998;47(9):1307–12.
[3] Kolokotsa D, Tsiavos D, Stavrakakis GS, Kalaitzakis K, Antonidakis E. Advanced fuzzy logic controllers design and evaluation for buildings' occupants thermal-visual comfort and indoor air quality satisfaction. Energy Build 2001;33:531–43.
[4] ISO 7730. Moderate thermal environments—determination of the PMV and PPD indices and specification of the conditions for thermal comfort. Geneva: International Organisation for Standardization; 1994.
[5] ANSI/ASHRAE Standard 55-2010. Thermal environmental conditions for human occupancy. Atlanta: American Society of Heating, Refrigerating, and Air-Conditioning Engineers Inc; 2010.
[6] Olesen BW. International standards for the indoor environment. Indoor Air 2004;14(Suppl. 7):18–26.
[7] Fanger PO. Thermal comfort: analysis and applications in environmental engineering. New York: McGraw-Hill; 1972.
[8] Fanger PO, Toftum J. Extension of the PMV model to non-air-conditioned buildings in warm climates. Energy Build 2002;34(6):533–6.
[9] De Dear RJ, Spagnolo J. Thermal comfort in outdoor and semi-outdoor environments. In: Tochihara Y, Ohnaka T, editors. Environmental ergonomics –

the ergonomics of human comfort, health and performance in the thermal environment. Elsevier Ltd; 2005. pp. 269–76.
[10] Liu W, Lian Z, Zhao B. A neural network evaluation model for individual thermal comfort. Energy Build 2007;39:1115–22.
[11] Stoops JL. Indoor thermal comfort, an evolutionary biology perspective. In: Proc. conference comf. energy use build – get them right. Windsor, UK: Cumberland Lodge; 27–30 April, 2006.
[12] Beccali M, Cellura M, Lo Brano V, Marvuglia A. Forecasting daily urban electric load profiles using artificial neural networks. Energy Convers Manag 2004;45(18/19):2879–900.
[13] Beccali M, Cellura M, LoBrano V, Marvuglia A. Short-term prediction of household electricity consumption: assessing weather sensitivity in a Mediterranean area. Renew Sustain Energy Rev 2008;12(8):2040–65.
[14] Marvuglia A, Messineo A. Using recurrent artificial neural networks to forecast household electricity consumption. Energy Procedia 2012;14:45–55.
[15] Yildiz Y, Arsan ZD. Identification of the building parameters that influence heating and cooling energy loads for apartment buildings in hot-humid climates. Energy 2011;36:4287–96.
[16] Messineo A, Marchese F. Performance evaluation of hybrid RO/MEE systems powered by a WTE plant. Desalination 2008;82:93–229.
[17] Messineo A, Panno D. Potential applications using LNG cold energy in Sicily. Int J Energy Res 2008;32:1058–64.
[18] Hassid S, Santamouris M, Papanikolaou M, Linardi A, Klitsikas N. The effect of the heat island on air conditioning load. Energy Build 2000;32(2):131–41.
[19] Beccali G, Cellura M, Culotta S, Lo Brano V, Marvuglia A. Set up of a monitoring system for a preliminary evaluation of the Urban Heat Island in the town of Palermo. In: Proc 25th passive and low energy architecture international conference (PLEA 2008), Dublin, Ireland October 22–24; 2008.
[20] Cellura M, Culotta S, Lo Brano V, Marvuglia A. Nonlinear black-box models for short-term forecasting of air temperature in the town of Palermo. In: Murgante B, Borruso G, Lapucci A, editors. Geocomputation, sustainability and environmental planning. Berlin/Heidelberg: Springer; 2011. pp. 183–204.
[21] Santamouris M, Papanikolaou N, Livada I, Koronakis I, Georgakis C, Assimakopoulos DN. On the impact of urban climate to the energy consumption of buildings. Sol Energy 2001;70(3):201–16.
[22] Cheng PJ, Cheng CH, Chang TS. Variant-frequency fuzzy controller for air conditioning driver by programmable logic controller. In: Proc 2011 8th Asian control conference (ASCC) Kaohsiung, Taiwan May 15–18; 2011. pp. 1159–63.
[23] Frontczak M, Wargocki P. Literature survey on how different factors influence human comfort in indoor environments. Build Environ 2011;46:922–37.
[24] Zalejska-Jonsson A, Wilhelmsson M. Impact of perceived indoor environment quality on overall satisfaction in Swedish dwellings. Build Environ 2013;63:134–44.
[25] Dounis AI, Tiropanis P, Argiriou A, Diamantis A. Intelligent control system for reconciliation of the energy savings with comfort in buildings using soft computing techniques. Energy Build 2011;43:66–74.
[26] Freire RZ, Oliveira GHC, Mendes N. Predictive controllers for thermal comfort optimization and energy savings. Energy Build 2008;40(7):1353–65.
[27] Calvino F, La Gennusa M, Rizzo G, Scaccianoce G. The control of indoor thermal comfort conditions: introducing a fuzzy adaptive controller. Energy Build 2004;36:97–102.
[28] Dounis AI, Manolakis DE. Design of a fuzzy system for living space thermal comfort regulation. Appl Energy 2001;69:119–44.
[29] Gouda MM, Danaher S, Underwood CP. Quasi-adaptive fuzzy heating control of solar buildings. Build Environ 2006;41:1881–91.
[30] Mustafaraj G, Lowry G, Chen J. Prediction of room temperature and relative humidity by autoregressive linear and nonlinear neural network models for an open office. Energy Build 2011;43:1452–60.
[31] Soleimani-Mohseni M, Thomas B, Fahlén P. Estimation of operative temperature in buildings using artificial neural networks. Energy Build 2006;38(6):635–40.
[32] Huang H, Chen L, Mohammadzaheri M, Hu E. A new zone temperature predictive modeling for energy saving in buildings. Procedia Eng 2012;49:142–51.
[33] Thomas B, Soleimani-Mohseni M. Neural network models for predictive climate control in intelligent buildings. In: ISAD04 conference, Budapest, Hungary 2004.
[34] Mechaqrane M, Zouak M. A comparison of linear and neural network ARX models applied to a prediction of the indoor temperature of a building. Appl Neural Comput 2004;13:32–7.
[35] Gouda M, Danaher S, Underwood CP. Application of an artificial neural network for modelling the thermal dynamics of a building's space and its heating system. Math Comput Model Dyn Syst 2002;8:333–44.
[36] Argiriou AA, Bellas-Velidis I, Balaras CA. Development of a neural network heating controller for solar buildings. Neural Netw 2000;13:811–20.
[37] Kusiak A, Xu G, Tang F. Optimization of an HVAC system with a strength multi-objective particle-swarm algorithm. Energy 2011;36:5935–43.
[38] Kusiak A, Xu G. Modeling and optimization of HVAC systems using a dynamic neural network. Energy 2012;42:241–50.
[39] Ben-Nakhi AE, Mahmoud MA. Energy conservation in buildings through efficient A/C control using neural networks. Appl Energy 2002;73(1):5–23.
[40] Stavrakakis GM, Zervas PL, Sarimveis H, Markatos NC. Optimization of window-openings design for thermal comfort in naturally ventilated buildings. Appl Math Model 2012;36:193–211.
[41] Stavrakakis GM, Karadimou DP, Zervas PL, Sarimveis H, Markatos NC. Selection of window sizes for optimizing occupational comfort and hygiene based on computational fluid dynamics and neural networks. Build Environ 2011;46:298–314.
[42] Homod RZ, Sahari KSM, Almurib HAF, Nagi FH. RLF and TS fuzzy model identification of indoor thermal comfort based on PMV/PPD. Build Environ 2012;49:141–53.
[43] Nørgaard M, Ravn O, Poulsen NK, Hansen LK. Neural networks for modelling and control of dynamic systems. London, UK: Springer-Verlag; 2000.
[44] Gautama T, Mandic DP, Van Hulle MM. A differential entropy based method for determining the optimal embedding parameters of a signal. In: Proc. ICASSP, vol. VI; 2003. pp. 29–32. Hong Kong.
[45] Gautama T. Optimal embedding parameters. Available online: http://webscripts.softpedia.com/-developer/Temu-Gautama-15893.html; 2007.
[46] Hagan MT, Menhaj M. Training feedforward networks with the Marquardt algorithm. IEEE Trans Neural Netw 1994;5(6):989–93.
[47] Beale MH, Hagan MT, Demuth HB. Neural network Toolbox™ 7 user's guide. The MathWorks Inc.; 2010.
[48] Mizumoto M, Tanaka K. Some properties of fuzzy sets of type-2. Inf Control 1976;31:312–40.
[49] Wag LX. A course on fuzzy systems and control. New Jersey: Prentice Hall; 1997.
[50] Takens F. Detecting strange attractors in turbulence. In: Rand DA, Young LS, editors. Dynamical systems and turbulence. New York: Springer; 1981. pp. 366–81.
[51] Beirlant J, Dudewicz EJ, Györfi L, van der Meulen EC. Nonparametric entropy estimation: an overview. Int J Math Stat Sci 1997;6:17–39.
[52] Schreiber T, Schmitz A. Surrogate time series. Physica D 2000;142:346–82.
[53] Rissanen J. Modeling by the shortest data description. Automatica 1978;14:465–71.
[54] Theiler J, Eubank S, Longtin A, Galdrikian B, Farmer JD. Testing for nonlinearity in time series: the method of surrogate data. Physica D 1992;58(1–4):77–94.